Beyond Tumors: Exploring Non-Neoplastic Renal Pathology

Alex McDonald, MD

Matthew Smith, MD, PhD

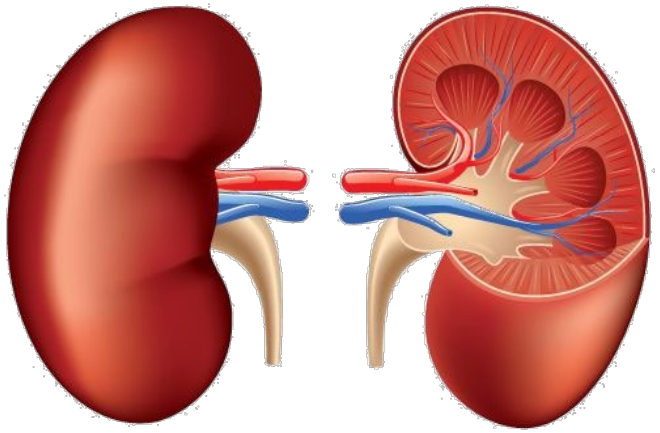

Objectives

1. Provide a broad overview of non-neoplastic renal pathologies to expand differential diagnosis.
2. Help differentiate between neoplastic and non-neoplastic renal pathologies.
3. Deepen knowledge of mass-like diseases to prevent unnecessary procedures and follow-up imaging.

Dromedary hump

- Thought to be caused by adaptation/molding of the kidney along the adjacent spleen
- Incidence of ~0.5%

- Imaging
  - Focal bulge on the lateral aspect of the **left** kidney
    - Can mimic a mass, particularly on ultrasound

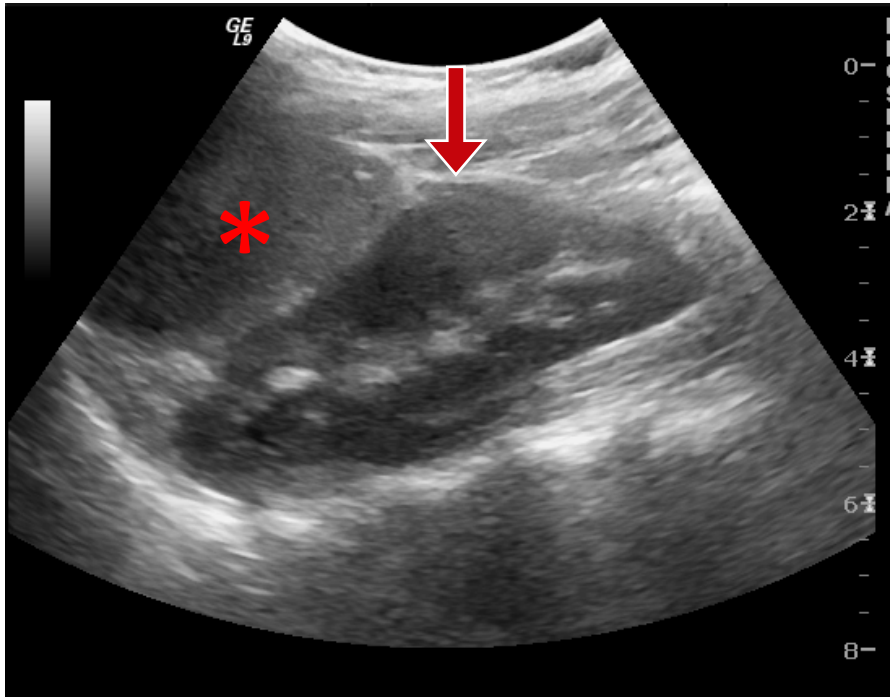

Dromedary hump (arrow) mimicking a hypoechoic mass on longitudinal ultrasound. Note the impression of the spleen (*) along the upper pole of the kidney.

Prominent/hypertrophied column of Bertin

- Hypertrophic cortical tissue extending toward the renal sinus
  - Typically in the middle ⅓ of the kidney
- Imaging
  - Identical enhancement and signal as adjacent cortex on CT and MRI
    - No bulging of the peripheral contour of the kidney
  - Can be more echogenic than adjacent renal cortex on US due to anisotropy

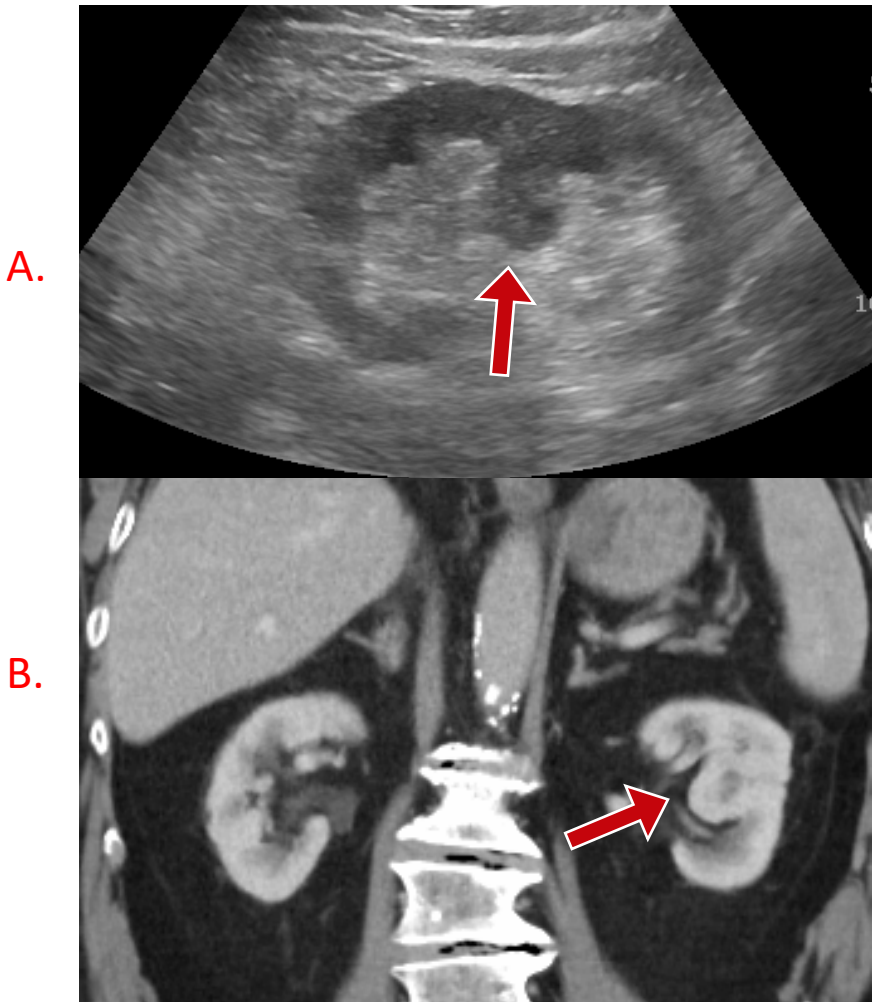

Longitudinal ultrasound (A) and coronal contrast-enhanced CT images (B) demonstrate hypertrophic cortical tissue (arrow) extending into the renal sinus. Note the lack of bugle along the renal capsule to help distinguish from mass.

Persistent fetal lobulation

- Embryologically, the kidney branches from a ureteric bud in a lobulated pattern
  - Each lobule consists of a medullary pyramid and a calyx
  - Lobulation typically resolves by the 3rd semester
- Imaging
  - Lobulated renal contour with indentations between pyramids
    - In contrast, scarring may indent the pyramid itself

A.

B.

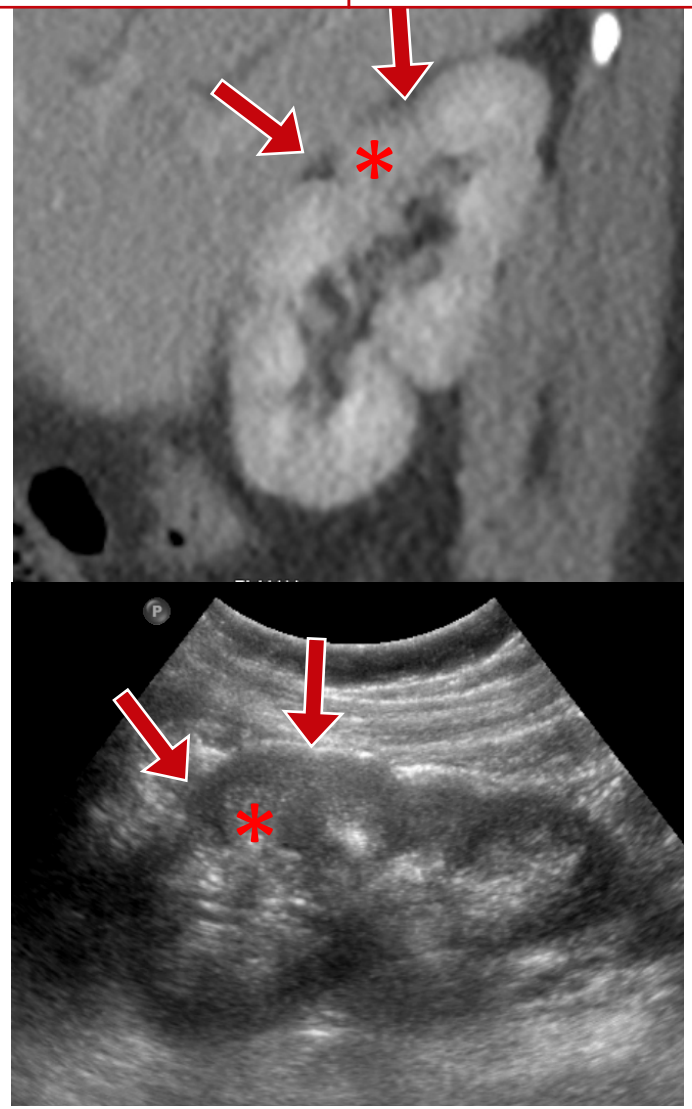

Sagittal contrast-enhanced CT (A) and longitudinal ultrasound (B) images demonstrate renal contour indentations (arrow) with sparing of the pyramids (*). Image A courtesy of Chris O'Donnell [1].

Junctional parenchymal defect

- Caused by incomplete fusion of renal lobules
- Imaging
  - Triangular-shaped defect typically at the junction of the upper and mid pole of the kidney
    - Represents renal sinus fat extending into the cortex

A.

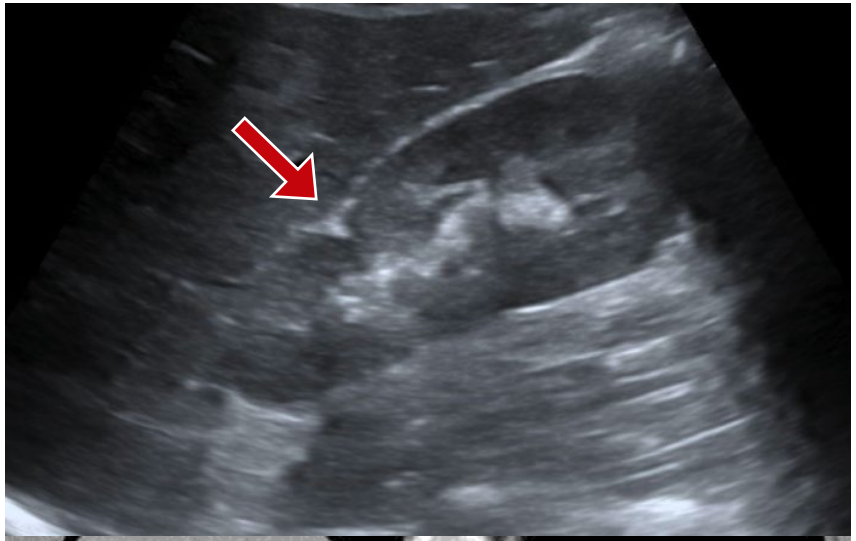

B.

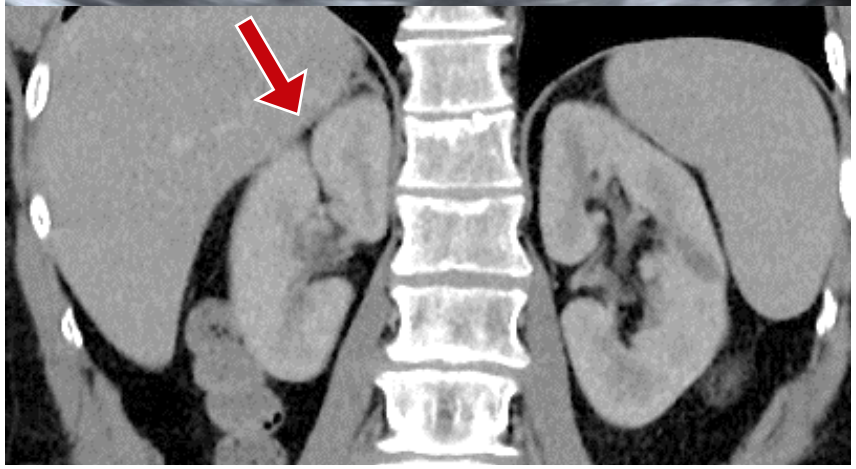

A. Longitudinal ultrasound demonstrates triangular shaped echogenic fat (arrow) extending into the cortex. B. Coronal contrast-enhanced CT shows hypodense fat (arrow) interposed between renal lobules. Image A courtesy of Ira Blau[2] and image B courtesy of Amir Rezaee[3].

Cystic disease

- Simple cysts
- Complex cysts
  - Hemorrhagic, proteinaceous
  - Septations, calcifications, enhancement
    - Bosniak classification for cystic renal masses
- Disease associated
  - VHL
    - Cysts are the most common visceral manifestation of disease (59-63%)
    - RCC (24%–45%) can arise de novo or from pre-existing cysts
      - Simple appearing cysts on imaging can contain foci of RCC which can grow over time and cause the original cyst to involute
  - Tuberous sclerosis
    - Most common manifestation is AML
    - Second is renal cysts

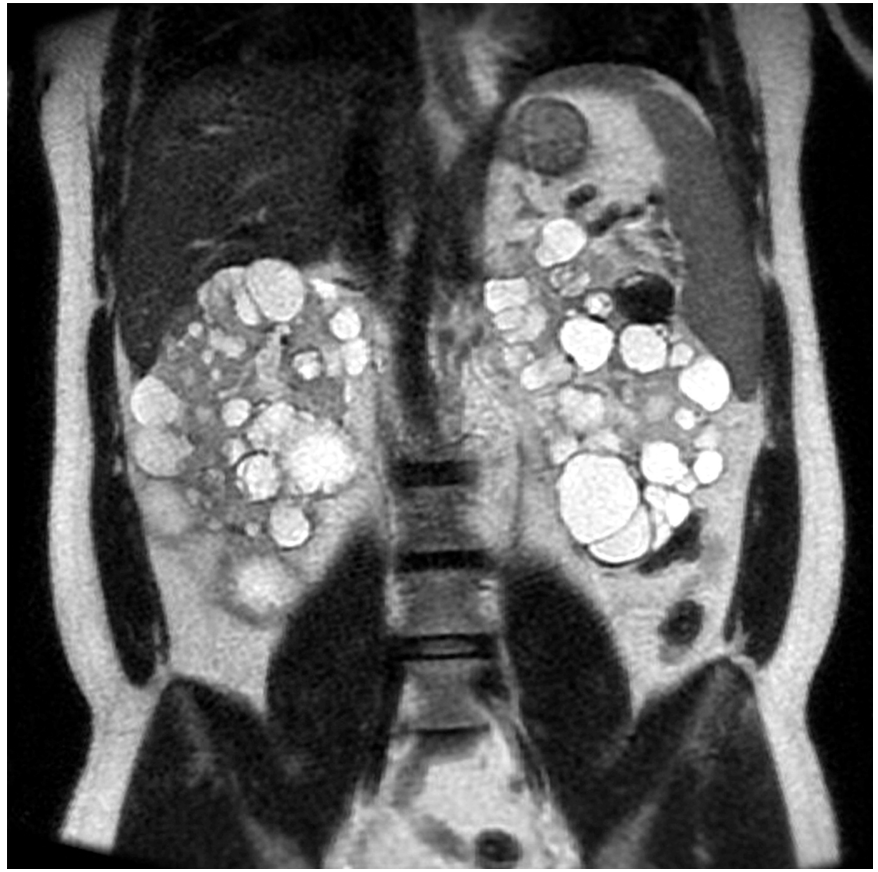

34-year-old with VHL. Coronal T2 weighted MRI demonstrates bilateral renal cysts of differing sizes. Case courtesy of D. Gaeshan et al.[4]

Lithium nephropathy

- Lithium is most commonly used to treat bipolar disorder
  - Causes ductal and tubule remodeling resulting in microcyst formation
  - Long-term use can cause chronic interstitial inflammation
- Imaging
  - Numerous 1-2 mm **microcysts** within the cortex and medulla, symmetrically distributed
  - Kidneys typically normal in size

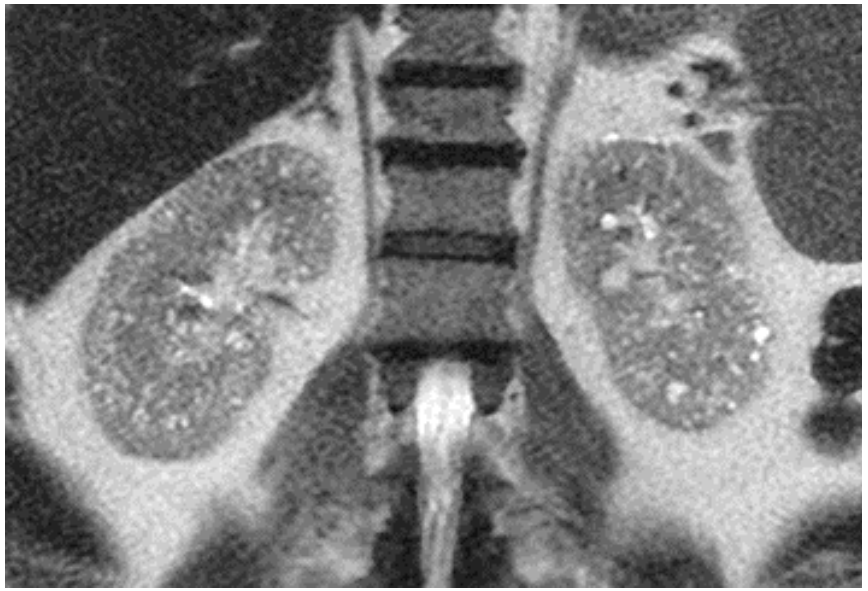

Coronal T2 weighted MRI demonstrates bilateral, symmetric microcysts in kidneys of normal size

Autosomal Dominant Polycystic Kidney Disease

- Most common genetic cause of renal failure worldwide
- Progressive renal cyst formation and kidney enlargement
  - Liver is the most common site of extrarenal involvement
- Imaging diagnostic criteria: number of cysts and familial history
- Renal complications
  - Cyst hemorrhage or superinfection
  - Nephrolithiasis
  - Hypertension
  - Renal failure

A. Coronal T2 weighted MRI with fat saturation demonstrates enlarged kidneys with numerous simple cysts (red arrow). Multiple cysts are also seen in the liver (*). B. Coronal FDG-PET/CT shows peripheral uptake in two renal cysts (white arrows) consistent with renal cyst superinfection.

Autosomal Recessive Polycystic Kidney Disease

- Patients present prenatally or in childhood
- Caused by renal tubal malformation and elongation resulting in non-obstructive dilation of the collecting system
  - Subsequent fibrosis causes renal enlargement
  - Ultimately leads to hypertension and renal failure
- Imaging findings
  - Enlarged kidney with microcysts < 2mm
  - US: Enlarged, **echogenic** kidneys with loss of corticomedullary differentiation
  - CT: Striated appearance due to contrast pooling within the dilated tubules
- Extra-renal manifestation
  - In the liver, bile ducts and portal tracts are also malformed resulting in congenital hepatic fibrosis

A.

B.

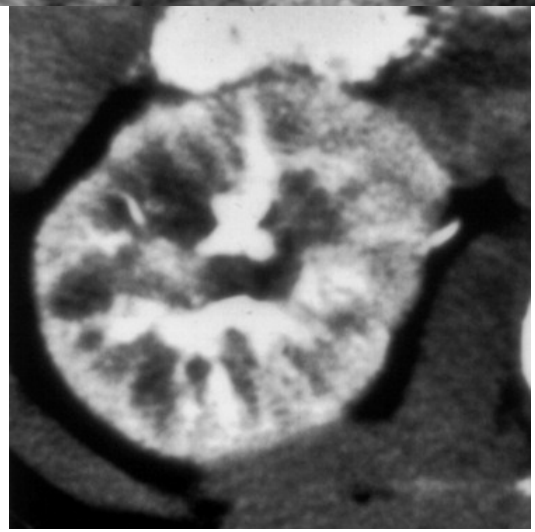

A. 3rd trimester longitudinal ultrasound shows loss of corticomedullary differentiation in an enlarged kidney (arrows). B. Excretory phase CT shows linear enhancement oriented in a radial fashion consistent with contrast pooling. Both images courtesy of Lonergan et al.[7]

Multicystic dysplastic kidney

- Thought to be secondary to failure of the ureteric bud to induce metanephric blastema differentiation resulting in cartilage, cyst, and disorganized tubule formation
- Typically diagnosed in childhood on ultrasound
  - Cluster of noncommunicating cysts replacing the normal renal parenchyma
- Usually regresses by adulthood but in a minority of cases, a residual mass remains within the renal fossa

A.

B.

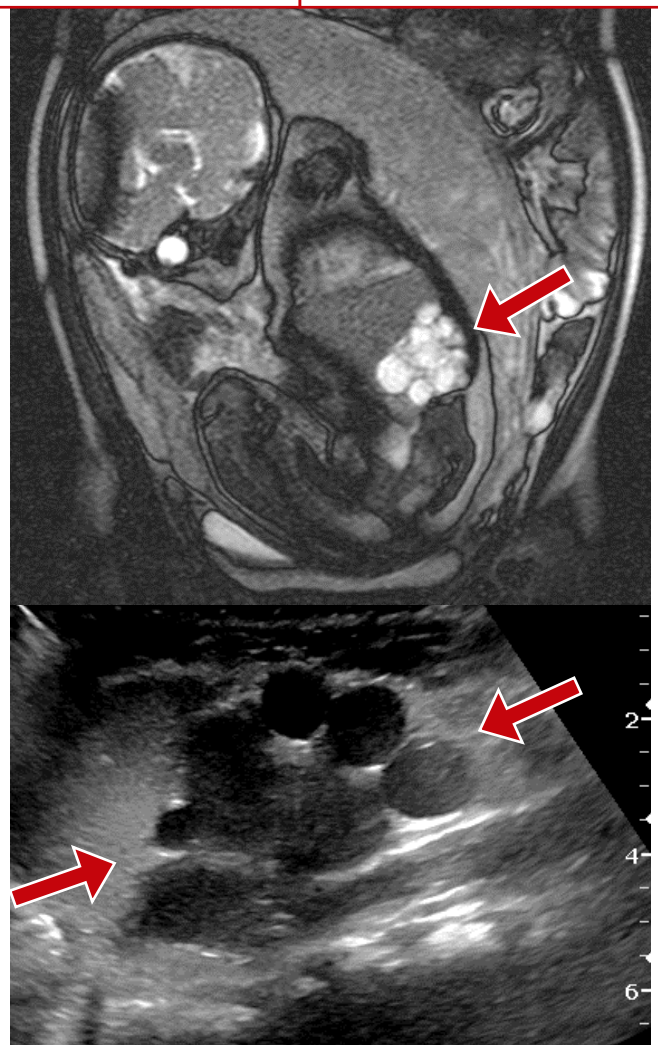

Prenatal coronal T2 fat saturated MRI (A) and longitudinal ultrasound (B) both show replacement of the right kidney with clustered cysts (arrow). Image A courtesy of G Balachandran[5].

Acquired cystic renal disease

- Development of at least 3 cysts in each kidney in patients with **end-stage renal disease on dialysis** without hereditary cystic disease
- Unclear etiology, likely multifactorial
  - Tubular obstruction and expansion fibrosis, hyperplasia, and increased fluid secretion
- Time on dialysis correlated with likelihood of disease
  - >10 years, ~100% acquire cystic renal disease
- Imaging
  - Small kidneys
  - Cysts are small, measuring < 3 cm
- Complications
  - Cyst hemorrhage
  - Increased risk of RCC

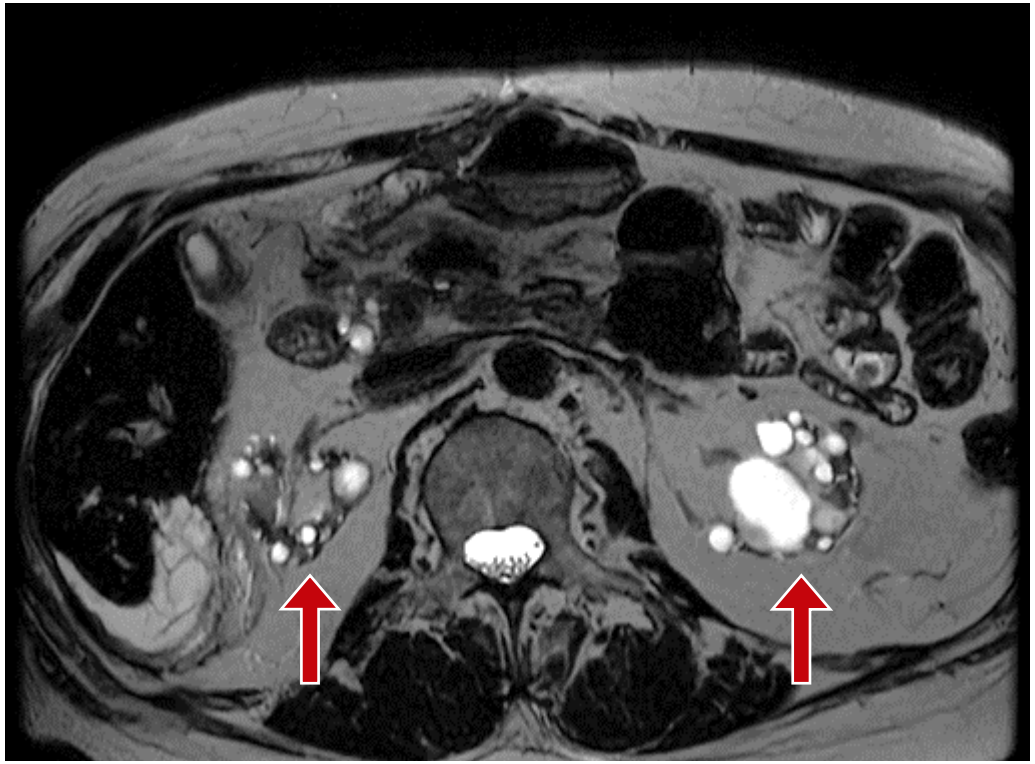

Axial 2D MRCP MRI demonstrates atrophic kidneys with numerous bilateral renal cysts (arrows).

Acute bacterial pyelonephritis

- Ascending urinary tract infection involving the renal parenchyma
  - Bacteria enter tubules at the papilla causing inflammation of the tubule that extends into the parenchyma
    - Causes wedge-shaped/linear hypoenhancement extending from the papilla to the renal cortex on imaging
      - **Becomes less defined as the infection continues**
    - Persistent enhancement on delayed imaging because contrast is not well excreted from these compromised tubules
    - Pattern can also be seen in nephritis caused by medication, granulomatous disease, and other less common disorders
- **Imaging lags clinical improvement and can take up to 5 months to resolve**

A.

B.

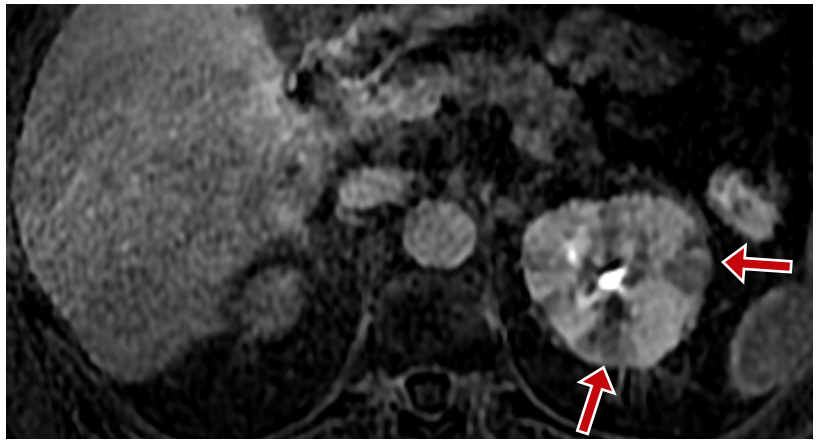

Axial contrast-enhanced CT (A) and MRI post-contrast MRI with fat saturation demonstrate multiple linear/wedge shaped areas of hypoenhancement (arrows) within the kidneys.

Pyelonephritis complication

- Lobar nephronia or acute focal nephritis
  - Intermediate stage between pyelonephritis and abscess
- Renal abscess
  - 75% of patients who develop abscesses have diabetes

A.

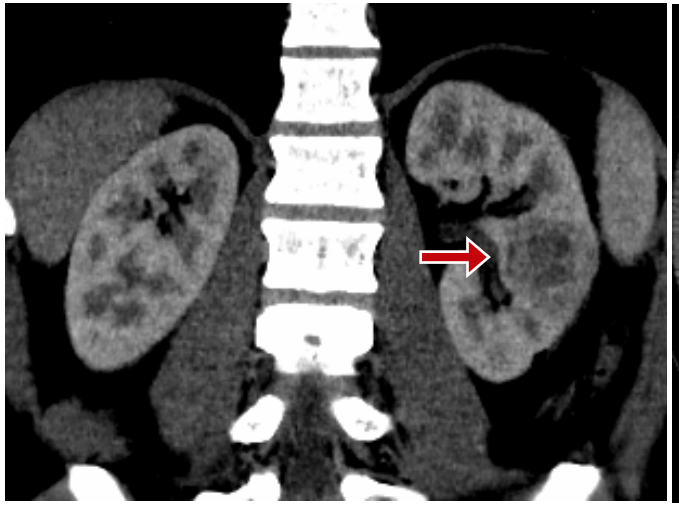

B.

C.

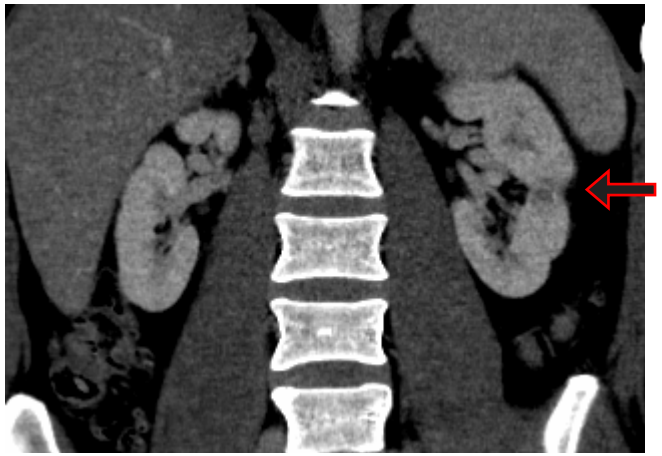

Coronal (A) and axial (B) contrast-enhanced CT images demonstrate a rim enhancing fluid collection (red arrow) with fluid-fluid level (white arrow). Follow-up CT (C) shows residual scar (black arrow).

Emphysematous pyelonephritis

- Life threatening infection caused by gas producing bacteria
- 90% patients have **poorly controlled DM**
- Imaging
  - Enlarged kidney with destruction of normal parenchyma
    - Foci or linear streaks of gas within the parenchyma
    - Fluid collections with gas-fluid levels
  - Gas within renal fossa or gas extending into the renal fascia indicates perinephric spread of infection

A.

B.

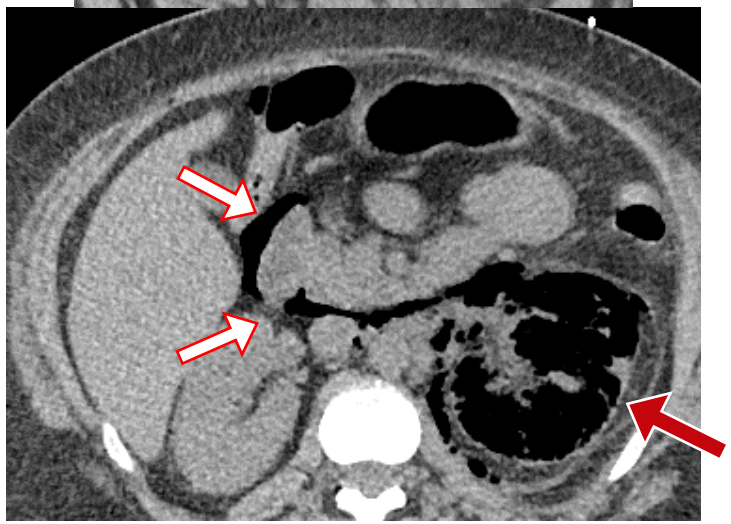

Coronal (A) and axial (B) non-contrast CT show an enlarged left kidney replaced with gas (red arrows) with gas extending into the retroperitoneum (white arrows).

Xanthogranulomatous pyelonephritis

- Chronic granulomatous destruction of the kidney secondary to recurrent bacterial infections
  - Parenchyma replaced by lipid-laden macrophages
- Imaging findings
  - Enlarged kidney with perinephric inflammation
  - Staghorn calculus
  - Calyceal dilation
  - No excretion on delayed imaging

A.

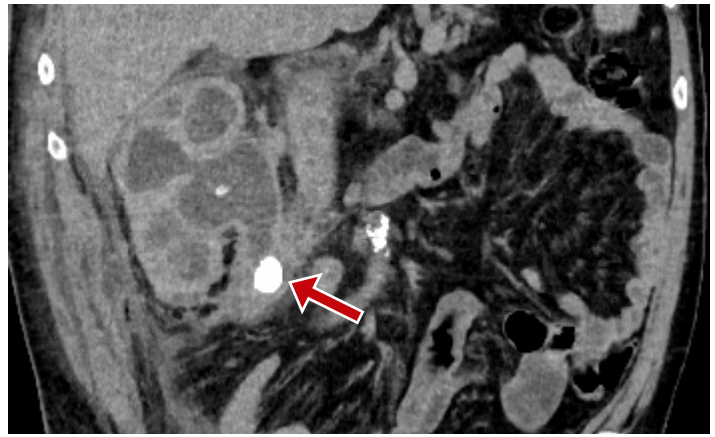

B.

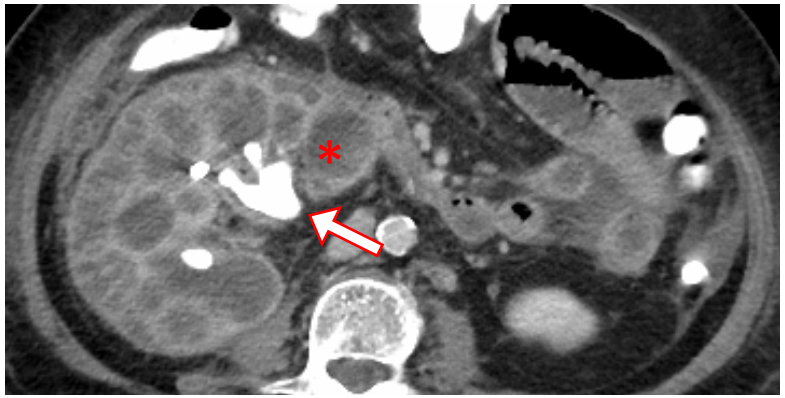

A. Coronal CT demonstrates obstructing stone in the proximal ureter (red arrow) with upstream hydroureteronephrosis. B. Axial CT shows staghorn calculus with calyceal dilation (*). Both kidneys are enlarged with surrounding inflammation.

Milk of Calcium

- Calcium precipitate layering dependently within a calyceal diverticulum or renal cyst
- Mimics renal stone or partially calcified renal cyst

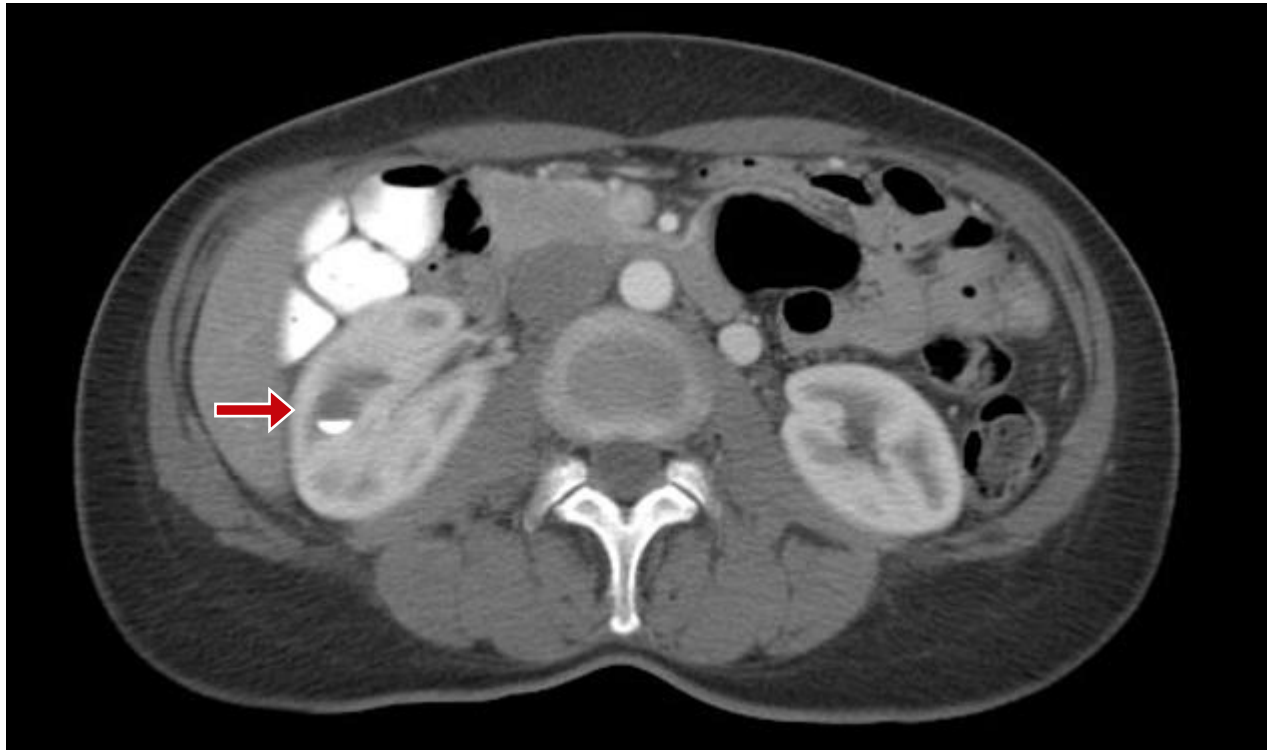

Calcium layering dependently in a calyceal diverticulum. Case courtesy of The Radswiki[6].

Medullary nephrocalcinosis

- Medullary nephrocalcinosis
  - CT: hyperdense medullary pyramids
  - US: echogenic pyramids with posterior shadowing
- Numerous causes
  - Diseases causing **elevated calcium or phosphate in the blood or urine**
    - Ex: Sarcoidosis, renal tubular acidosis, medullary sponge kidney
  - Rare, hereditary causes
    - Ex: Lowe Disease, Dent disease

A.

B.

Coronal contrast-enhanced (A) and non-contrast (B) CT images in different patients show bilateral calcification in the medullary pyramids (arrows).

Medullary sponge kidney

- **Congenital** abnormality resulting in cystic dilation of the medullary connecting ducts
  - Results in urinary stasis and predisposition to calcium precipitation
- Medullary nephrocalcinosis pattern
  - Bilateral in 70% of cases
    - Asymmetrically affects the kidneys and may be segmental or involve a single medullary pyramid

A.

B.

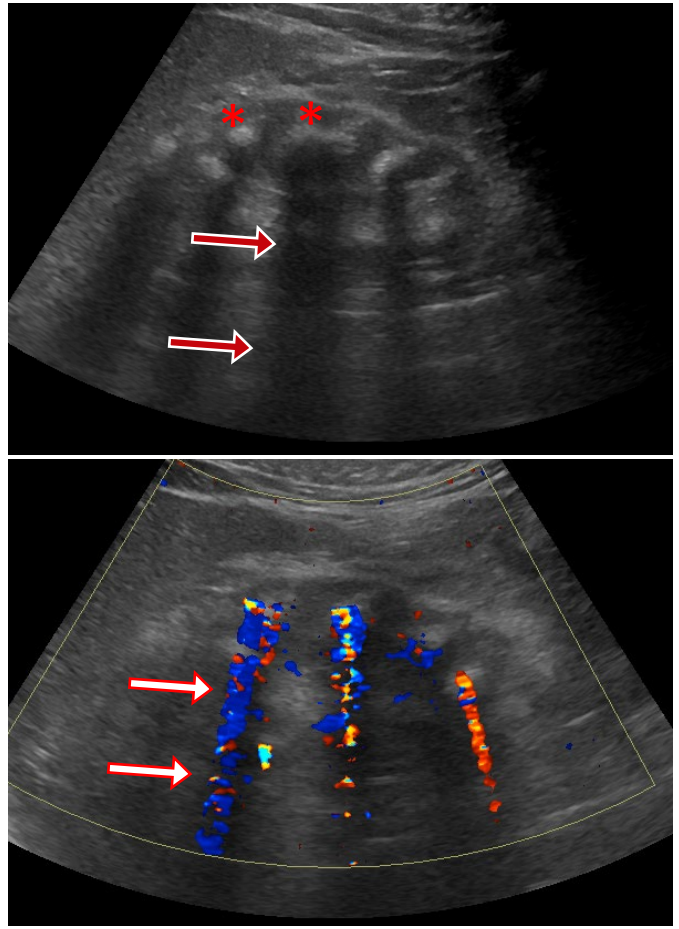

A. Longitudinal ultrasound shows hyperechoic medullary pyramids (*) with posterior shadowing (red arrows). B. Longitudinal ultrasound with color doppler demonstrates “twinkle” artifact (white arrows).

Cortical nephrocalcinosis

- Causes
  - Chronic glomerulonephritis
  - Chronic renal transplant rejection
  - Sequelae of acute cortical necrosis
  - Rare genetic syndromes such as Alport Syndrome
- Imaging
  - Calcification within the renal cortex

A.

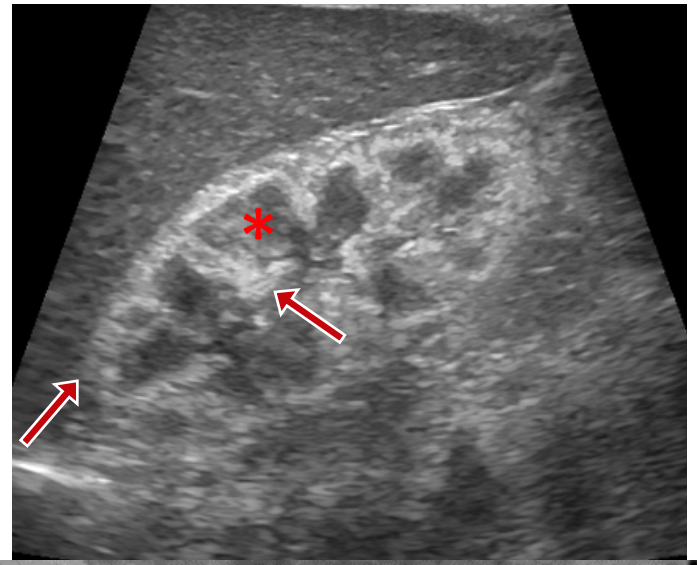

B.

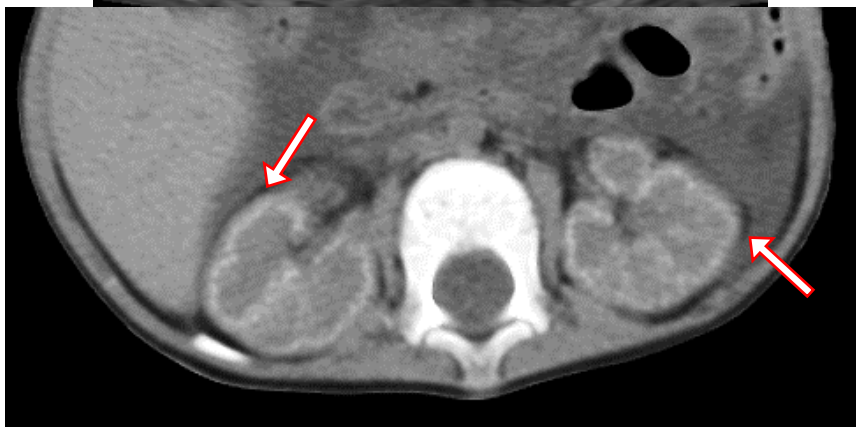

A. Longitudinal ultrasound shows hyperechoic renal cortex (red arrow). Note the hypoechoic medullary pyramids (*). B. Axial non-contrast CT shows hyperdense renal cortex (white arrow) with normal medullary pyramids. Both images courtesy of Mahmoud Mekhaimar.[8]

Trauma

- Renal injury
  - American Association for the Surgery of Trauma (AAST) renal injury scale
  - Hematoma → Page kidney
    - Subcapsular hematoma or collection causing **hypertension** by activation of the renin-angiotensin-aldosterone system due to renal hypoperfusion

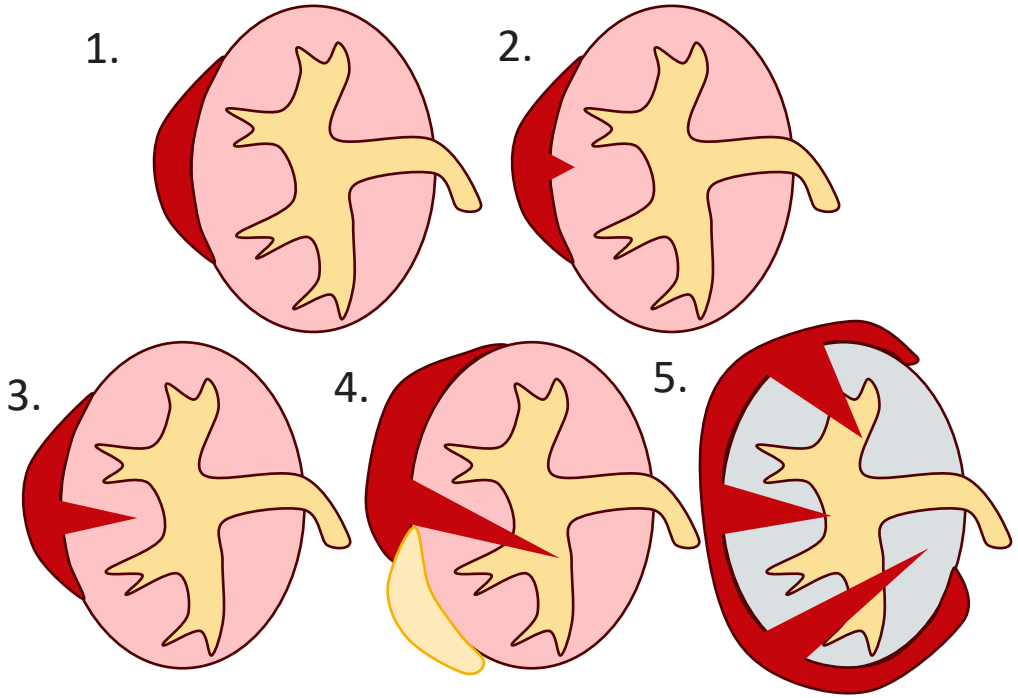

Simplified diagram and criteria of the AAST renal injury scale.

- Grade 1: Subcapsular hematoma without laceration.
- Grade 2: Laceration ≤1 cm in depth
- Grade 3: Laceration > 1 cm in depth without involvement of the collecting system.
- Grade 4: Laceration **involving the collecting system** with evidence of urine leak.
- Grade 5: Shattered or devascularized kidney

Trauma continued…

A.

B.

C.

AAST Grade 4 renal injuries

A. Coronal CT demonstrates renal **lacerations** (red arrow) within the mid and lower poles with associated **subcapsular hematoma** (*).

B. Follow-up excretory phase CT shows **infarct** in the mid to lower pole (red arrow) with evolving hematoma (*).

C. Coronal CT shows lacerations within the left upper pole (red arrow) and associated **renal vein thrombosis** (white arrow). Note the splenic lacerations (black arrow).

Infarct

- Complete or partial occlusion of the main renal artery or one of its branches
  - Most common cause is embolism from the heart (55%) or in-situ thrombus
- Imaging
  - Wedge-shaped hypoenhancement
  - Cortical rim sign only seen in about 50% of cases and typically several days after infarct

A.

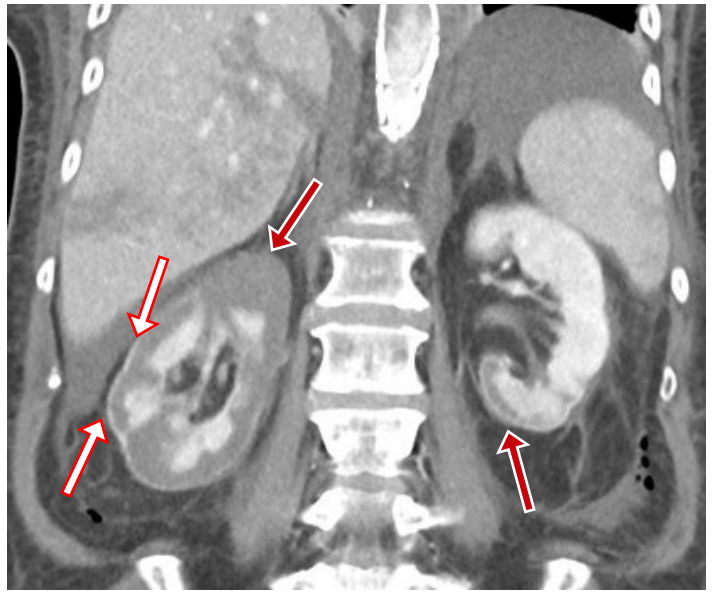

B.

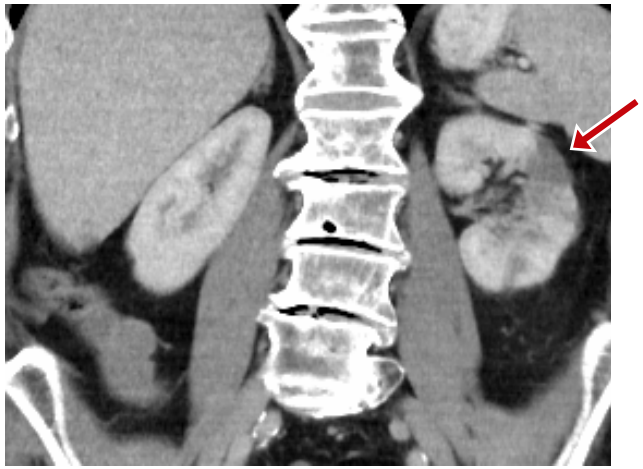

C.

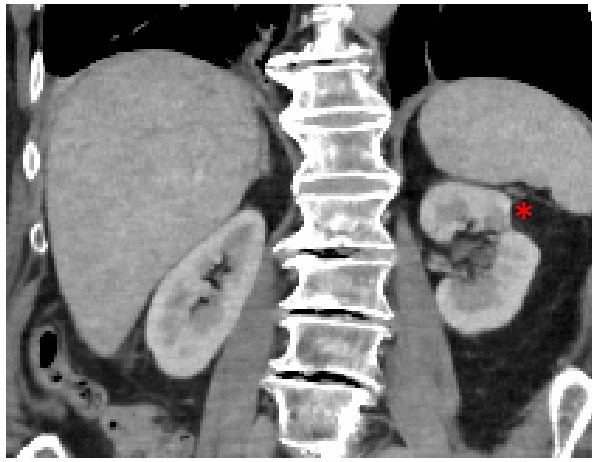

A. Coronal CT shows multifocal infarcts in both kidneys (red arrows). Persistent cortical enhancement of the left kidney consistent with "cortical rim sign" (white arrows). Note the additional infarcts within the liver and spleen. B, C. Coronal CT shows multifocal infarcts in the left kidney (red arrow) with residual scar (*). Image A courtesy of Bruno Di Muzio.[9]

Renal cortical necrosis

- Mechanism
  - Poorly understood
  - Ultimately thought to be from diminished arterial perfusion of the renal cortex secondary to vasospasm, injury, or intravascular coagulation
- Imaging
  - Hypoenhancement of the renal cortex
  - Normal enhancement of the medulla

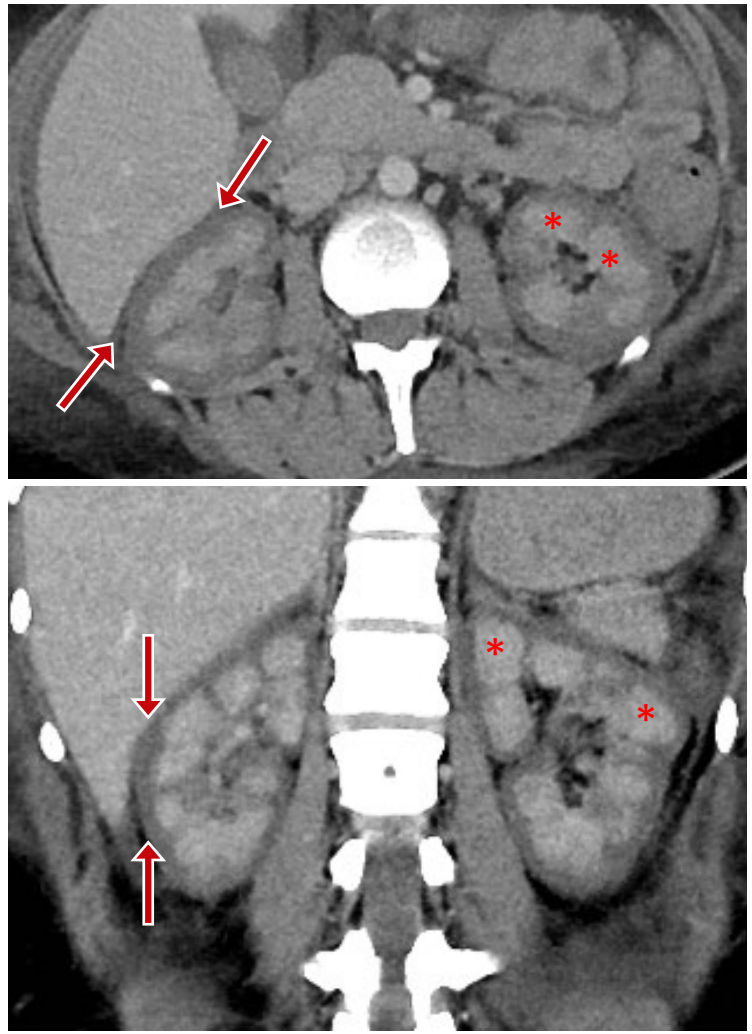

A, B. Axial and coronal contrast-enhanced CTs show hypoenhancement of the renal cortex (arrows) with normal enhancement of the medullary pyramids (*). Both cases courtesy of Hsu.[10]

Renal papillary necrosis

- Medulla and papilla are at risk for ischemia due to slow blood flow to the vasa recta and relative hypertonic environment
- Multiple etiologies
  - Diabetes, sickle cell disease, pyelonephritis, obstructive uropathy, amongst others
- Imaging
  - Early: ill defined hypoenhancement at the tips of the medullary pyramids
  - Late: ischemia papillae slough leading to calyceal deformity
  - Patterns
    - Medullary: central necrosis at the tip of the pyramid resulting in a round/oval cavity
    - Papillary: a larger portion of the papilla necroses resulting in a triangular defect
      - "lobster claw sign"
  - **Most identifiable on urographic phase** when contrast fills the papillary defects, demonstrating the ischemic/destructive process

A.

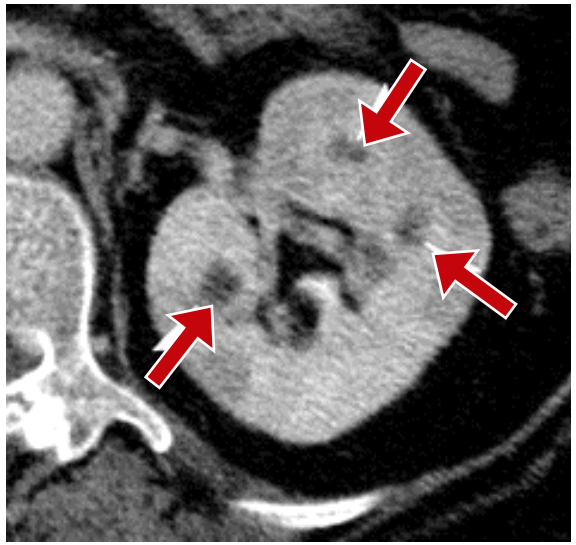

B.

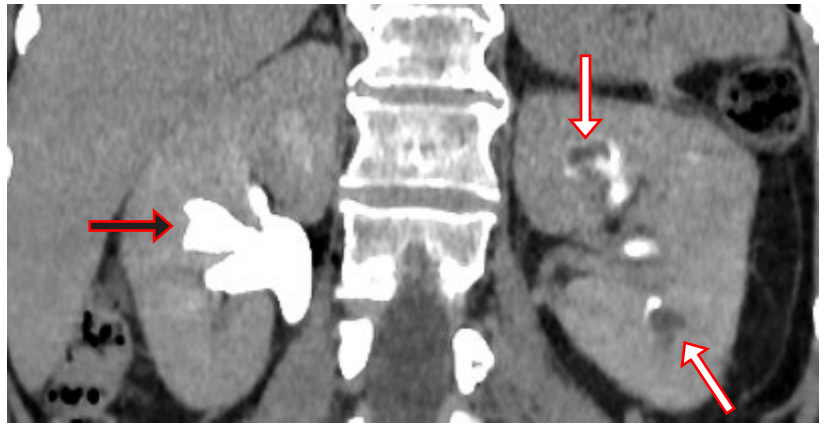

A. Axial CT shows early ischemia of the renal papilla (red arrows). B. Coronal urographic phase CT shows multiple filling defects within the left kidney from sloughed papillae (white arrows) and blunted calyces within the right kidney (black arrow). Image A courtesy of Dae Chul Jung et al[29] and Image B courtesy of Ashesh Ranchod.[11]

Aneurysm and Pseudoaneurysm

- Aneurysm: abnormal dilation of the vessel wall
- True aneurysm
  - All layers of the wall are intact (intima, media, adventitia)
  - 90% are extra-parenchymal
  - Most common causes: atherosclerosis, **fibromuscular dysplasia**
  - Imaging: Fusiform or saccular dilation of a vessel
- Pseudoaneurysm
  - Most common causes: penetrating trauma, iatrogenic injury
  - Direct vessel injury causes extravasated blood to leak and be **contained by the media or adventitia**
  - US: cystic structure connected to a feeding artery by a neck of variable length
    - Turbulent flow: "yin-yang sign"

A.

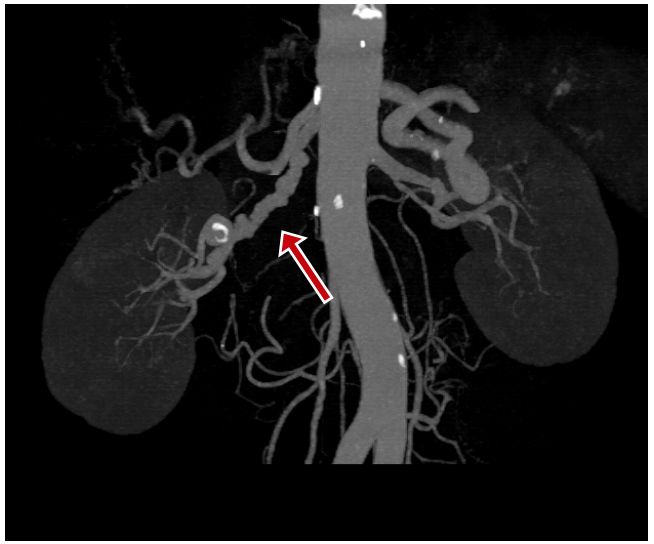

B.

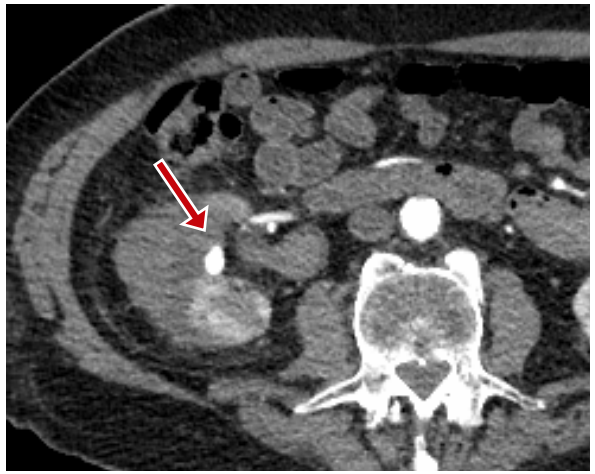

C.

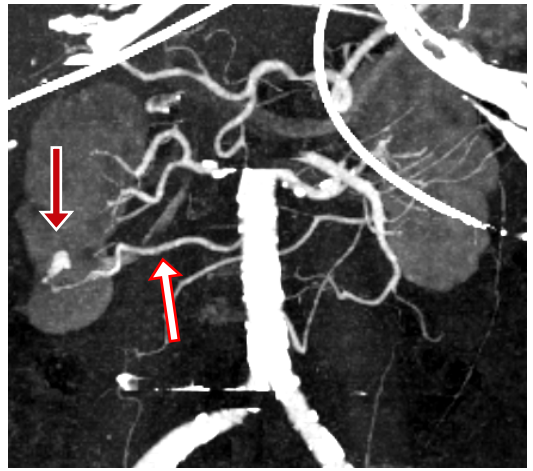

A. 3D MIP demonstrates fibromuscular dysplasia affecting the right (arrow) greater than left renal arteries. B. Axial arterial phase CT shows right lower pole pseudoaneurysm as a complication of microwave ablation. C. 3D MPR of the same patient shows an accessory renal artery (white arrow) feeding the pseudoaneurysm (red arrow).

Renal AVM

- Arteriovenous malformation (AVM) and arteriovenous fistula (AVF) represent an abnormal communication between a renal artery and vein
- AVM and AVF differences
  - AVM is primarily congenital
    - Hereditary Hemorrhagic Telangiectasia
  - AVF is typically acquired
    - Trauma, iatrogenic from biopsy or surgery
  - **AVM has a vascular nidus, AVF does not**
- Imaging findings
  - US: hypoechoic structure in the parenchyma can mimic mass
  - CT/MRI: enhances with blood pool
    - Early enhancement of the draining vein
  - AVM: vascular nidus

A.

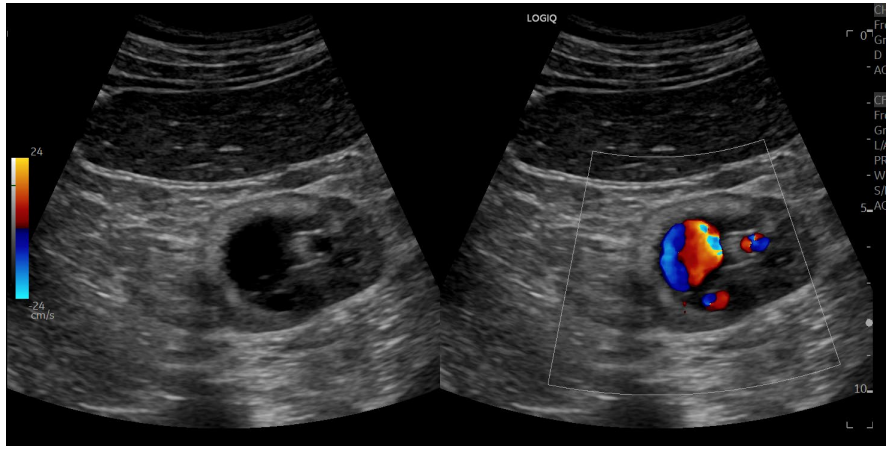

B.

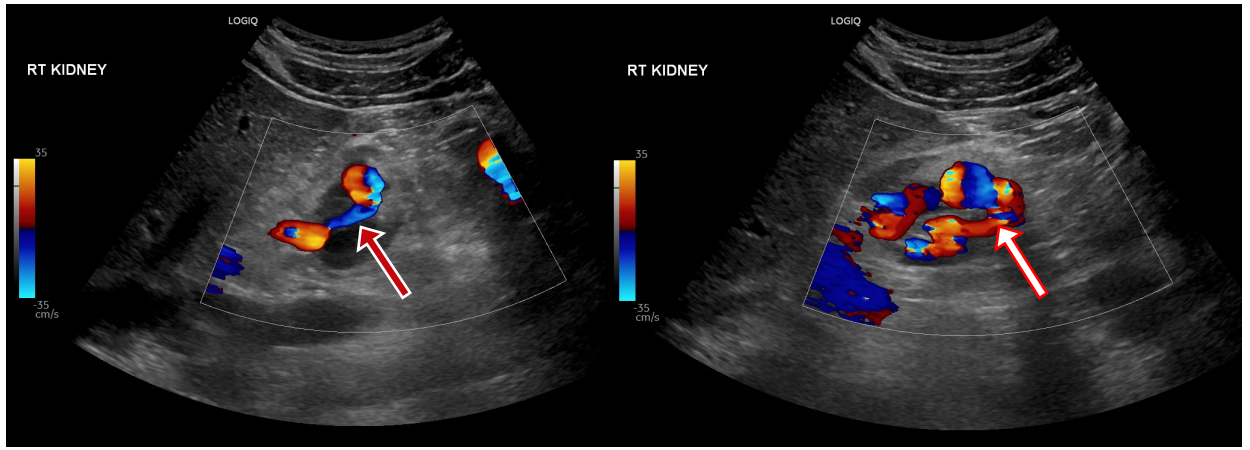

A. Longitudinal ultrasound of the right kidney shows a complex cystic structure with internal blood flow representing a vascular nidus. B. Doppler ultrasound demonstrates a feeding artery (red arrow) and enlarged draining vein (white arrow) with arterial waveforms (not shown).

Conclusion

- Broadening the differential for a radiologist can help improve clinical care and management decision making.
- Accurate diagnosis of infection and trauma can help guide medical and interventional treatment options.
- Knowing mimics of cancer in the kidneys can prevent avoidable work-up, biopsy, and follow-up imaging.

References

1. Chris O'Donnell. Persistent Fetal Renal Lobulation. https://radiopaedia.org/cases/persistent-fetal-renal-lobulation/
2. Ira Blau et al. Incidentalomas among healthy nephrology fellow Volunteers at POCUS Workshops: A case series – POCUS Journal. https://pocusjournal.com/article/2022-07-kidney-p30-32/
3. Amir Rezaee. Junctional Parenchymal Defect of Kidney. https://radiopaedia.org/cases/junctional-parenchymal-defect-of-kidney
4. Ganeshan D, Menias CO, Pickhardt PJ, et al. Tumors in von Hippel–Lindau Syndrome: From Head to Toe—Comprehensive State-of-the-Art Review. Radiographics. 2018;38(3):849-866. doi:10.1148/rg.2018170156
5. G Balachandran. Multicystic dysplastic kidney (antenatal MRI). https://radiopaedia.org/cases/multicystic-dysplastic-kidney-antenatal-mri
6. The Radswiki. Calyceal diverticulum. https://radiopaedia.org/cases/calyceal-diverticulum
7. Lonergan GJ, Rice RR, Suarez ES. Autosomal Recessive Polycystic kidney Disease: Radiologic-Pathologic correlation. Radiographics. 2000;20(3):837-855. doi:10.1148/radiographics.20.3.g00ma20837
8. Mahmoud Ibrahim Mekhaimar. Bilateral renal cortical calcification. https://radiopaedia.org/cases/bilateral-renal-cortical-calcification
9. Bruno Di Muzio. Multiple abdominal viscera thromboembolic infarcts. https://radiopaedia.org/cases/multiple-abdominal-viscera-thromboembolic-infarcts
10. Charlie Chia-Tsong Hsu. Renal cortical necrosis. https://radiopaedia.org/cases/renal-cortical-necrosis
11. Ashesh Ishwarlal Ranchod. Renal papillary necrosis. https://radiopaedia.org/cases/renal-papillary-necrosis-3
12. Koratala, A., & Bhattacharya, D. (2018, June 13). *Kidney hump, no need to jump!*. Clinical case reports. https://www.ncbi.nlm.nih.gov/pmc/articles/PMC6099045/
13. Oktay Algin, Evrim Ozmen, Mehmet Gumus. Hypertrophic Columns of Bertin: Imaging findings. https://www.eajm.org/en/hypertrophic-columns-of-bertin-imaging-findings-1617140
14. Bhatt S, MacLennan G, Dogra V. Renal pseudotumors. American Journal of Roentgenology. 2007;188(5):1380-1387. doi:10.2214/ajr.06.0920
15. Syed Muhammad Nazim, Muhibullah Bangash, and Basit Salam. Persistent fetal lobulation of kidney mimicking renal tumour. https://www.ncbi.nlm.nih.gov/pmc/articles/PMC5747680/

References continued...

16. Carter AR, Horgan JG, Jennings TA, Rosenfield AT. The junctional parenchymal defect: a sonographic variant of renal anatomy. Radiology. 154(2):499-502. doi:10.1148/radiology.154.2.3880914
17. Farres MT, Ronco P, Saadoun D, et al. Chronic lithium nephropathy: MR imaging for diagnosis. Radiology. 2003;229(2):570-574. doi:10.1148/radiol.2292020758
18. Lerma, Edgar V. Renal toxicity of lithium. https//www.uptodate.com/contents/renal-toxicity-of-lithium
19. Wood CG, Stromberg LJ, Harmath CB, et al. CT and MR Imaging for Evaluation of Cystic Renal Lesions and Diseases. Radiographics. 2015;35(1):125-141. doi:10.1148/rg.351130016
20. Mahboob M, Rout P, Leslie SW, Bokhari SRA. Autosomal dominant polycystic kidney disease. StatPearls - NCBI Bookshelf. Published March 20, 2024. https://www.ncbi.nlm.nih.gov/books/NBK532934/
21. Lonergan GJ, Rice RR, Suarez ES. Autosomal Recessive Polycystic kidney Disease: Radiologic-Pathologic correlation. Radiographics. 2000;20(3):837-855. doi:10.1148/radiographics.20.3.g00ma20837
22. Wood CG, Stromberg LJ, Harmath CB, et al. CT and MR Imaging for Evaluation of Cystic Renal Lesions and Diseases. Radiographics. 2015;35(1):125-141. doi:10.1148/rg.351130016
23. Craig WD, Wagner BJ, Travis MD. Pyelonephritis: Radiologic-Pathologic Review. Radiographics. 2008;28(1):255-276. doi:10.1148/rg.281075171
24. Naeem M, Zulfiqar M, Siddiqui MA, et al. Imaging manifestations of genitourinary tuberculosis. Radiographics. 2021;41(4):E1123-E1143. doi:10.1148/rg.2021200154
25. Yeh HC, Mitty HA, Halton K, Shapiro R, Rabinowitz JG. Milk of calcium in renal cysts: new sonographic features. Journal of Ultrasound in Medicine. 1992;11(5):195-203. doi:10.7863/jum.1992.11.5.195
26. Vaidya PN, Rathi BM, Finnigan NA. Page Kidney. StatPearls - NCBI Bookshelf. Published January 22, 2023. https://www.ncbi.nlm.nih.gov/books/NBK482486/#:~:text=Page%20kidney%20or%20Page%20phenomenon,%2Daldosterone%20system%20(RAAS).
27. Saju JM, Leslie SW. Renal infarction. StatPearls - NCBI Bookshelf. Published March 10, 2024. https://www.ncbi.nlm.nih.gov/books/NBK582139/
28. Prakash J, Singh VP. Changing picture of renal cortical necrosis in acute kidney injury in developing country. World Journal of Nephrology. 2015;4(5):480. doi:10.5527/wjn.v4.i5.480
29. Jung DC, Kim SH, Jung SI, Hwang SI, Kim SH. Renal Papillary Necrosis: Review and comparison of findings at Multi–Detector Row CT and Intravenous Urography. Radiographics. 2006;26(6):1827-1836. doi:10.1148/rg.266065039
30. Cura M, Elmerhi F, Bugnogne A, Palacios R, Suri R, Dalsaso T. Renal aneurysms and pseudoaneurysms. Clinical Imaging. 2011;35(1):29-41. doi:10.1016/j.clinimag.2009.12.001
31. Mukendi et al. Renal arteriovenous malformation: An unusual pathology. https://www.ncbi.nlm.nih.gov/pmc/articles/PMC6837781/